

# Dynamo action due to spatially dependent magnetic permeability

To cite this article: B. Gallet *et al* 2012 *EPL* **97** 69001

View the [article online](#) for updates and enhancements.

## Related content

- [Effect of magnetic boundary conditions on the dynamo threshold of von Kármán swirling flows](#)  
C. Gissinger, A. Iskakov, S. Fauve et al.
- [A numerical model of the VKS experiment](#)  
C. J. P. Gissinger
- [Instabilities on a turbulent background](#)  
Stéphane Fauve, Johann Herault, Guillaume Michel et al.

## Recent citations

- [Effect of fluctuations on mean-field dynamos](#)  
A. Alexakis *et al*
- [Instabilities on a turbulent background](#)  
Stéphane Fauve *et al*
- [Exact two-dimensionalization of low-magnetic-Reynolds-number flows subject to a strong magnetic field](#)  
Basile Gallet and Charles R. Doering

# Dynamo action due to spatially dependent magnetic permeability

B. GALLET, F. PÉTRÉLIS and S. FAUVE

*Laboratoire de Physique Statistique, École Normale Supérieure, CNRS, Université P. et M. Curie, Université Paris Diderot - 24 rue Lhomond, F-75005 Paris, France, EU*

received 22 December 2011; accepted in final form 22 February 2012

published online 21 March 2012

PACS 91.25.Cw – Origins and models of the magnetic field; dynamo theories

PACS 47.65.-d – Magnetohydrodynamics and electrohydrodynamics

**Abstract** – We show that a simple flow of an electrically conducting fluid along a boundary with variable magnetic permeability can generate a magnetic field. An analytic study in the limit of weak permeability modulation allows to understand the mechanism of this dynamo and predicts scaling laws for the threshold. We discuss the possible contribution of this mechanism to the dynamo observed in the von Karman sodium experiment and we propose two flow configurations that could lead to the experimental observation of this new type of dynamo.

Copyright © EPLA, 2012

The magnetic field of many planets and stars is generated by the motion of an electrically conducting fluid through the dynamo process, an instability that converts flow kinetic energy into magnetic energy [1]. Several attempts of displaying this effect in laboratory experiments have only led to three successful results so far. In the Karlsruhe [2] and Riga [3] experiments, the flow lines have been strongly constrained by the boundaries in order to mimic laminar flows known for their dynamo efficiency. The kinetic Reynolds number of these liquid-sodium flows being large (in the range  $10^5$ – $10^6$ ), small-scale turbulent fluctuations could not be avoided but were much smaller than the mean flow. The geometry of the magnetic field observed in the Karlsruhe and Riga experiments, as well as the nature of the bifurcation to the dynamo regime, were in excellent agreement with predictions made using the mean-flow component alone, thus discarding turbulent fluctuations. By contrast, the von Karman sodium (VKS) experiment was designed with the aim of studying the dynamo process in a strongly turbulent flow [4]. To wit, a liquid-sodium flow driven by two counterrotating impellers in a cylinder has been chosen (see fig. 1). These von Karman swirling flows involve strong turbulent fluctuations, in particular when the impellers are in counterrotation, which generates a strong shear in the mid-plane. Although the kinetic Reynolds number achieved in the VKS experiment is only slightly larger than in the Karlsruhe and Riga experiments, turbulent fluctuations are as large as the mean flow and the geometry of the generated mean magnetic field (an axial dipole) [5] cannot be explained taking into account the mean flow alone. It has been

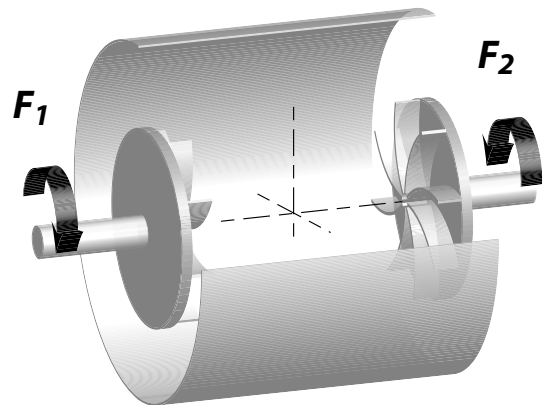


Fig. 1: Sketch of the VKS experiment. Two counterrotating disks drive a turbulent flow in around 160 L of liquid sodium. The disks are fitted with blades. Dynamo action is observed when a propeller is made of soft iron. A spatial modulation of the magnetic permeability is due to the blades.

proposed that non-axisymmetric velocity fluctuations in the form of vortices along the blades of the propellers induce an alpha effect, that together with differential rotation generates an alpha-omega dynamo [6]. Numerical simulations taking into account this non-axisymmetric velocity component in addition to the mean flow [7] or using a mean-field induction equation including an alpha effect [8] have strengthened this picture. Indeed, the axial dipolar magnetic field generated with counterrotating impellers, as well as the field reversals observed when the impellers are counterrotated at different frequencies [9], have been numerically simulated in ref. [7]. However,

ferromagnetic impellers have been modeled as boundaries of infinite magnetic permeability and the ferromagnetic blades of the impellers have not been taken into account.

Although we expect the VKS flow to generate a magnetic field also when non-magnetic impellers are used, a dynamo has been observed so far in the accessible range of rotation frequency only when both the disk and the blades of an impeller are made of iron [10]. It is thus clear that the dynamo threshold is lower in the presence of ferromagnetic blades. It has been proposed that the azimuthal modulation of the magnetic permeability related to the blades (see fig. 1) contributes to dynamo action [11] in a way similar to the one described by Busse and Wicht, who showed that a uniform flow over an infinite plate with spatially varying electrical conductivity is able to generate magnetic field [12].

The aim of this letter is twofold: first, we show how a spatial modulation of a solid boundary's magnetic permeability can turn a non-dynamo flow into a flow capable of dynamo action. Solving the equivalent of the Busse and Wicht model analytically in the case of a weak modulation of magnetic permeability allows to understand the mechanism of this class of dynamos and to predict scaling laws for the threshold, including the case of time-dependent dynamos that was previously discarded. Second, we want to determine whether this type of dynamo mechanism can operate in the range of magnetic Reynolds number accessible in the VKS experiment. This issue remaining questionable, we propose simple experimental configurations to test this mechanism.

We consider the simplest configuration that involves shear and spatial modulation of magnetic permeability, as presented in fig. 2. A fluid of electrical conductivity  $\sigma$  and magnetic permeability  $\mu_0$  flows uniformly with a velocity  $U\mathbf{e}_x$  in the semi-infinite space  $z > 0$ . A rigid boundary is located under the fluid. It has the same electrical conductivity as the fluid, and its magnetic permeability is  $\mu_0 \mu_r(\tilde{x})$ , with  $\mu_r(\tilde{x}) = m_0 + m_1 \sin(\tilde{x}/L)$ . This modulated boundary extends down to  $\tilde{z} = -DL$ , under which is a medium of infinite magnetic permeability. The boundary is not moving so that a shear is localized at  $z = 0$ . Numerical computations have been performed in a similar configuration where the magnetic permeability of the boundary is constant while the electrical conductivity is modulated in space [12].

We use  $L$  and  $\mu_0 \sigma L^2$  as length and time scales, and define the magnetic Reynolds number as  $Rm = \mu_0 \sigma UL$ . Denoting without a tilde the dimensionless coordinates, the induction equation inside the fluid reads

$$\partial_t \mathbf{B} + Rm \partial_x \mathbf{B} = \nabla^2 \mathbf{B}. \quad (1)$$

Inside the modulated boundary, the Maxwell-Faraday equation together with Ohm's law yields:

$$\mu_r \partial_t \mathbf{H} = -\nabla \times (\nabla \times \mathbf{H}), \quad (2)$$

with  $\mathbf{B} = \mu_0 \mu_r \mathbf{H}$ . Everywhere the magnetic field  $\mathbf{B}$  is divergence free. This set of equations is supplemented with

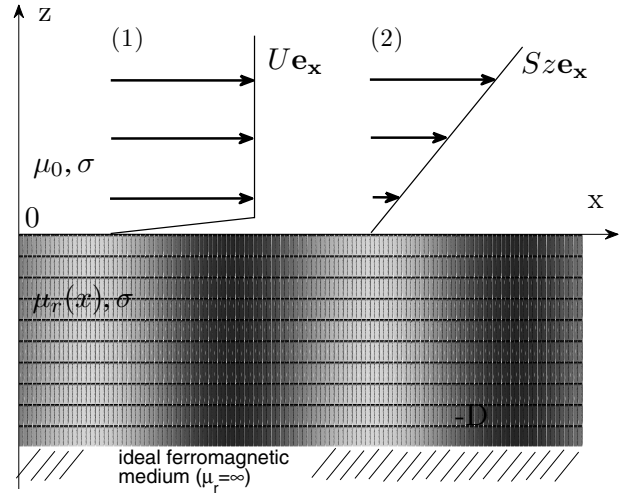


Fig. 2: Sketch of the flow and of the boundary of modulated magnetic permeability. Two flows are considered: (1) a uniform flow for  $z > 0$  with a shear localized at  $z = 0$ ; (2) a uniform shear.

matching conditions that relate the fields between the different domains. At the boundary  $z = -D$ , the perfect ferromagnetic medium imposes  $H_x = H_y = 0$  and  $\partial_z H_z = 0$ . At  $z = 0$ , the normal component of  $\mathbf{B}$ , the tangential ones of  $\mathbf{H}$  and of the electric field  $\mathbf{E} = (\nabla \times \mathbf{H})/\sigma - \mathbf{v} \times \mathbf{B}$  are all continuous.

Using translational invariance in the  $y$ -direction, we search for modes proportional to  $\exp(st +iky)$ . A dynamo mode is linearly unstable when the real part of the eigenvalue  $s$  becomes positive. To determine the value of  $s$  as a function of the problem's parameters  $Rm$ ,  $k$ ,  $m_0$ ,  $m_1$ , we Fourier transform the fields in the  $x$ -direction. In the fluid the different Fourier components are not coupled. The matching conditions at  $z = 0$  can then be written as two boundary conditions that constrain the field inside the boundary (*i.e.*, for  $-D \leq z \leq 0$ ). We then have to solve eq. (2) together with the boundary conditions at  $z = 0$  and  $z = -D$ . The problem is discretized in the  $z$ -direction using  $P$  uniformly spaced grid points. The generalized linear eigenvalue problem is thus written as a square matrix of dimension  $(2N + 1)^2(2P + 1)^2$  where we truncate the Fourier expansion in  $x$  at order  $N$ . For sufficiently large  $N$  and  $P$  (depending on the intensity of the magnetic permeability gradients), the eigenvalue  $s$  is converged.

The first result is that this configuration leads to dynamo instability: provided  $Rm$  is large enough, the magnetic permeability modulation together with the flow destabilizes a magnetic mode. We plot in fig. 3 the critical magnetic Reynolds number as a function of the relative permeability modulation  $m_r = m_1/(m_0 - 1)$ . We assume that the boundary is nowhere diamagnetic, so that  $\mu_r$  has to be everywhere higher than unity and the quantity  $m_r$  varies between 0 and 1: no permeability modulation gives  $m_r = 0$ , while a maximum permeability modulation

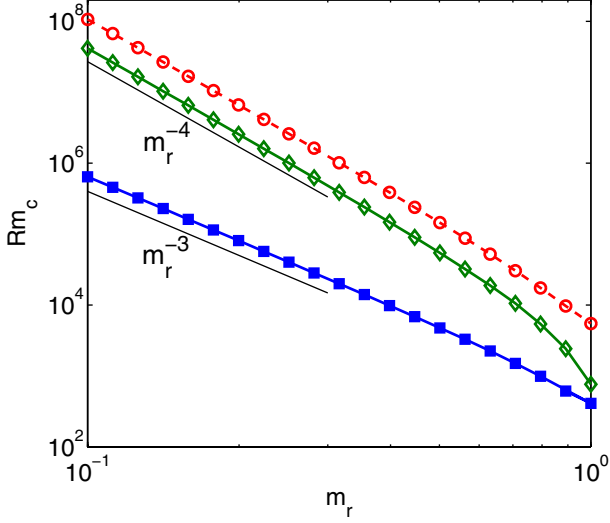


Fig. 3: (Colour on-line) Critical magnetic Reynolds number as a function of  $m_r$  for the onset of dynamo action for  $D = 1$ . Empty symbols are for the uniform flow (1) and full symbols for the shear flow (2); ( $\circ$ ):  $m_0 = 10$ ; ( $\diamond$ ):  $m_0 = 100$ , ( $\blacksquare$ ):  $m_0 = 100$ . The wave number  $k_c$  at onset ranges between 0.5 and 3: the eigenmode inside the boundary then has a typical lengthscale of order  $L$  in all 3 directions.

$\mu_r = m_0 + (m_0 - 1)\sin(x)$  corresponds to  $m_r = 1$ . We observe that the stronger the permeability modulation, the lower the dynamo onset. As this modulation goes to zero, the critical  $Rm$  diverges as  $m_r^{-4}$ , in agreement with an antidynamo theorem that holds for 2D flows with uniform magnetic permeability. For a fixed value  $m_r$ , the dynamo onset decreases toward a finite limit when  $m_0$  increases. We notice that the first unstable eigenmode is oscillatory for high values of  $m_0$  and low values of  $m_r$ , whereas it is stationary when  $m_r$  gets close to 1. The parameter space is thus quite rich as will be revealed by the small  $m_r$  asymptotic expansion.

To discuss the effect of the width of the boundary, we show in fig. 4 the onset of stationary dynamo action as a function of  $D$  for  $m_r = 1$ .  $Rm_c$  is a decreasing function of  $D$ . For large enough  $D$  the onset tends to a constant. Indeed, inside the boundary the magnetic field then extends on a dimensionless vertical lengthscale of about 1 and is thus not affected by the idealized ferromagnetic boundary at  $z = -D \ll -1$ . In line with this observation, note also that qualitatively similar results have been obtained if vacuum is considered at  $z < -D$  instead of ideal ferromagnetic material.

The problem simplifies in the limit of weak magnetic permeability modulation. We write  $\mu_r = m_0(1 + \epsilon \sin(x))$ , so that  $m_r = \epsilon m_0 / (m_0 - 1)$ , and consider  $\epsilon \ll 1$ . In this limit the eigenmode is dominated by a large-scale field (meaning independent of  $x$ ) and a harmonic component ( $\cos x$  and  $\sin x$  dependence). The latter is much weaker than the large-scale component: it comes from the effect of the magnetic permeability modulation on the large-scale

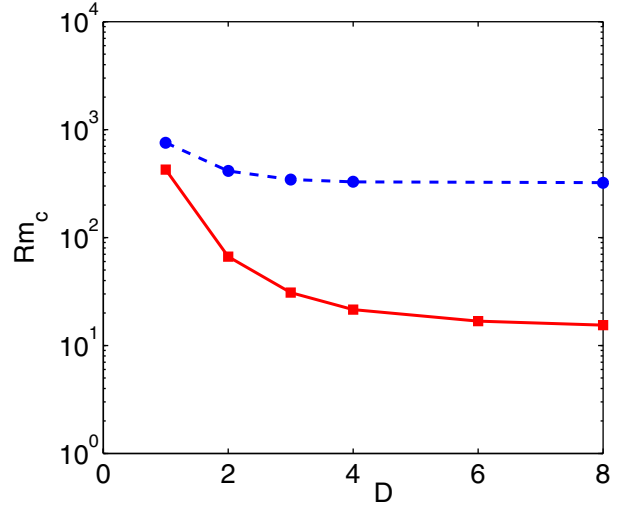


Fig. 4: (Colour on-line) Critical magnetic Reynolds number as a function of the width of the boundary  $D$  for  $m_0 = 100$  and  $m_r = 1$ . The dashed line joins results for flow (1) and the continuous line for flow (2).

field, and is thus  $\epsilon$  times smaller. The eigenmode has a scale separation in the  $x$ -direction that makes possible an asymptotic expansion. We decompose the fields into two components:  $H_x = H_x(z) + h_x(x, z)$  and  $H_z = H_z(z) + h_z(x, z)$  where  $H_x$  and  $H_z$  are the large-scale components and  $h_x$  and  $h_z$  are the harmonic components. The field in the  $y$ -direction can be obtained using the divergence-free condition for  $\mathbf{B}$ . The problem involves six unknowns: the amplitudes of the large-scale fields  $H_x$  and  $H_z$  and the amplitudes of the two quadratures of  $h_x$  and  $h_z$ . Boundary conditions result in a linear system of six equations, the determinant of which vanishes when  $s$  is an eigenvalue. At the dynamo onset, the real part of  $s$  vanishes and its imaginary part is the pulsation at onset. This asymptotic approach confirms the numerical results presented in fig. 3: for a weak modulation of magnetic permeability, we find the same magnetic Reynolds numbers, wave numbers and pulsations at criticality. More generally, three modes are in competition. One is oscillatory and two are stationary. The stationary or oscillatory nature of the first unstable mode depends on the position in the  $(D, m_0)$ -plane. The parameter space contains three domains separated by several boundaries corresponding to codimension-2 bifurcations where the modes exchange stability.

The neutral mode for  $m_r = 1$  is drawn in fig. 5. This drawing, together with the asymptotic expansion allows to understand the physical mechanism of this dynamo. This mechanism can be described in four steps that are sketched in fig. 6. Let us assume that there is a large-scale field  $H_x(z)$  in the vicinity of the boundary. Without magnetic permeability modulation such a field can verify the equations and matching conditions at the boundary. However, if the magnetic permeability of the boundary has variations in  $x$ , the divergence-free

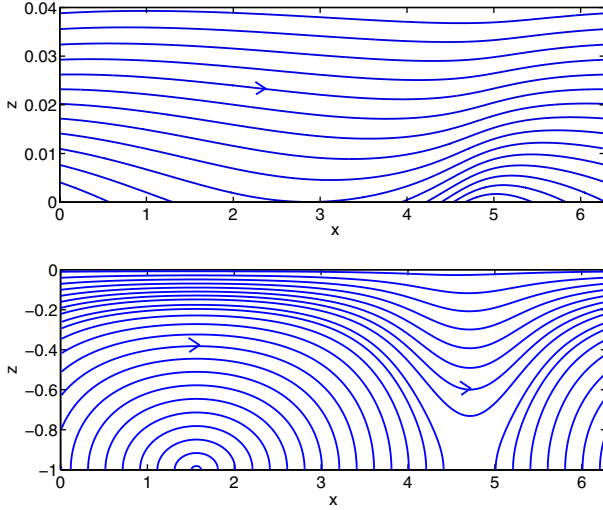


Fig. 5: (Colour on-line) Magnetic-field lines projected in the  $(x, z)$ -plane for  $m_0 = 10$ ,  $m_r = 1$ ,  $D = 1$  and at the onset of instability for the uniform flow (1). Top: in the flow; bottom: in the boundary. Note the very different  $z$ -scales of the two panels: the skin effect inside the fluid concentrates the  $x$ -dependent field very close to the boundary.

constraint for  $\mathbf{B}$  requires a non-zero small-scale field in the vertical direction, of order  $h_1 \simeq \epsilon H_x$ . The permeability modulation thus induces a small-scale vertical magnetic field which originates from canalization of the magnetic field by the regions of large magnetic permeability. At step (2), the shear flow localized close to the solid boundary converts this component into a component in the  $x$ -direction, say  $h_2$ . At  $z = 0$ , the boundary condition gives approximately  $\sqrt{Rm}h_2 \simeq h_1$ . This balance traces back to the usual skin effect: in a frame moving with the fluid at velocity  $U\mathbf{e}_x$ , the field that comes out of the boundary is an oscillatory field that penetrates into the fluid only in a skin layer, the depth of which is of order  $Rm^{-1/2}$ .

At the third step, the tangential component  $h_2$  interacts once again with the permeability modulation to produce a large-scale field:  $H_z \simeq \epsilon h_2$ . Finally, this field  $H_z$  is sheared, which generates a large-scale field along  $x$  through the  $\omega$ -effect:  $H_x \simeq Rm H_z$ . To sum up, this mechanism can be written as a cycle:  $H_x \simeq Rm H_z \simeq Rm \epsilon h_2 \simeq \sqrt{Rm} \epsilon h_1 \simeq \sqrt{Rm} \epsilon^2 H_x$ . At onset, the gain of this cycle is of order unity, which gives  $Rm \simeq \epsilon^{-4}$ .

We think that a similar mechanism is involved when a modulation of electrical conductivity is considered instead of a modulation of magnetic permeability. Then, the concentration of currents in the domains of large conductivity converts the tangential field into a normal one. We point out that the critical Reynolds number extracted from the results of [12] diverges as  $\epsilon^{-4}$  in agreement with the scaling presented here.

At this stage, the dynamo mechanisms do not seem to be very efficient. The critical Reynolds number remains larger than a few hundreds, which corresponds to unachievable velocities for a liquid-metal experiment. This high critical

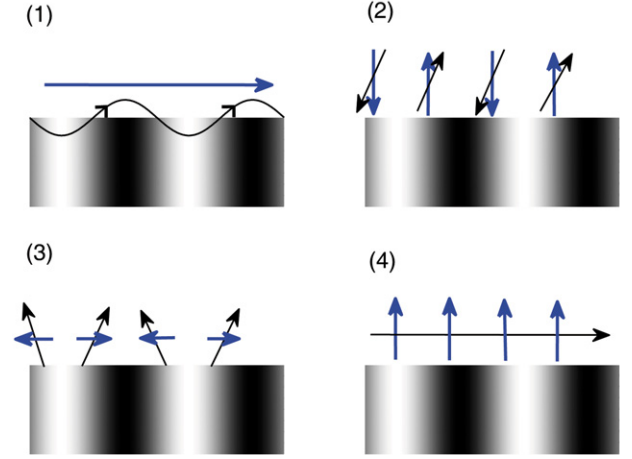


Fig. 6: (Colour on-line) Sketch of the effects involved in the dynamo process. At steps (1) and (3), the tangential component (thick blue line) is converted into a normal one (thin black line) by the modulation of magnetic permeability in the boundary. At steps (2) and (4), the normal component (thick blue line) created at the former step is converted into a tangential one (thin black line) by the shear. In the boundary, white colour stands for large permeability.

$Rm$  results from the expulsion by the skin effect of the modulated field generated in the boundary. To moderate this effect, we have slightly modified the system and have studied a linear shear (see fig. 1 (2)). We consider the velocity field  $\mathbf{u} = (Sz, 0, 0)$  and define the magnetic Reynolds number as  $Rm = \mu_0 \sigma SL^2$ . Both the numerical and the asymptotic calculations can be modified to tackle this geometry.

A dynamo magnetic field is generated above a critical magnetic Reynolds number  $Rm_c$  displayed as a function of  $D$  in fig. 4. Values of the order of 15 are reached. It is of course not straightforward to compare the numerical values of  $Rm_c$  in both geometries since the definitions are different. However, the linear shear is more efficient in the following sense. Because the fluid velocity is small close to the boundary, the skin effect is reduced compared to the case of a localized shear. Thus, the resulting field expulsion is not as intense and the induction cycle is more efficient. The low modulation asymptotic expansion and the numerical computations displayed in fig. 3 show that  $Rm_c \propto \epsilon^{-3}$  for  $\epsilon \ll 1$ . The change of exponent from  $-4$  to  $-3$  directly results from the weaker skin effect. Indeed, for a linear shear, the skin depth scales as  $Rm^{-1/3}$ , so that the second step of the mechanism results in  $h_2 \propto Rm^{-1/3} h_1$  from which the exponent  $-3$  is obtained for  $Rm_c$  [13].

From the point of view of the large-scale field, the mechanisms of instability at work in these dynamos can be described as the two following effects. A usual  $\omega$ -effect due to the shear converts the poloidal field (normal to the boundary) into a toroidal one (tangential). The second step is completely different from the one at work in usual dynamos ( $\omega$ -effect in the Lowes and Wilkinson dynamo [14],  $\alpha$ -effect in traditional geophysical and

astrophysical models). Indeed, it is the interplay between the shear and the ferromagnetic modulation that converts the toroidal component back into a poloidal one. This effect is sufficient to release the constraint of antidynamo theorems. Here the flow is a very simple two-dimensional field and yet a dynamo is observed. As expected, when the modulation vanishes the dynamo onset diverges.

This effect is possibly involved in the VKS dynamo. It may either be the dominant mechanism that converts the toroidal field into a poloidal field, or it may cooperate with the  $\alpha$ -effect generated by the vortices along the blades [6]. The results of the present letter can be compared to the VKS experiment only under the very crude assumptions that the turbulent von Karman flow can be replaced by a solid disk of modulated magnetic permeability close to which is the time-averaged shear in azimuthal velocity. The VKS impellers have radius  $R = 15.45$  cm with 8 blades of height 4.0 cm, which yields a characteristic length  $L = R/8 \sim 2$  cm. Because of the blades, we consider that the mean azimuthal velocity drops on a typical axial length comparable to the blades' height as we move away from the disk. This gives  $S \sim 500 \text{ s}^{-1}$  and a magnetic Reynolds number  $\mu_0 \sigma S L^2 \sim 2$ . This value is lower than the threshold of order 10 reported for  $m_0 = 100$  and  $m_r = 1$  that are values expected for the VKS disks. A better description of the geometry of the flow and impellers, as well as a precise knowledge of the magnetic permeability of the VKS disks would be necessary for further comparison.

A clear experimental demonstration of this new kind of dynamos thus remains necessary, and we now describe experiments specifically designed to isolate and measure the amplitude of the conversion of toroidal to poloidal magnetic field induced by a spatial variation of magnetic permeability. The disks in the VKS experiment are fitted with iron blades which are responsible for the azimuthal modulation of magnetic permeability. When the disk rotates, the blades increase the driving of the fluid in comparison with a flat disk. Turbulent fluctuations are more intense and the power required to drive the disk at a given angular velocity is thus strongly increased. A simple way to reduce the power required to drive the flow is to insert the ferromagnetic blades inside the disk. This suppresses the vortices along the blades but maintains the modulation of magnetic permeability. In other words, starting from the usual disks, we fill the space between the blades with a solid metal such as copper. The system is adjusted so that the disk's surface is flat, see fig. 7 (left). Therefore, for a given available mechanical power, the achievable rotation rate will be strongly increased. Close to the disk's surface both the modulation of magnetic permeability and the shear will be strong.

Another geometry that can be considered is inspired by the Taylor-Couette flow and is presented in fig. 7 (right). We consider two coaxial cylinders that can rotate independently. One or both of the cylinders' surfaces are machined to insert axial pieces of ferromagnetic material.

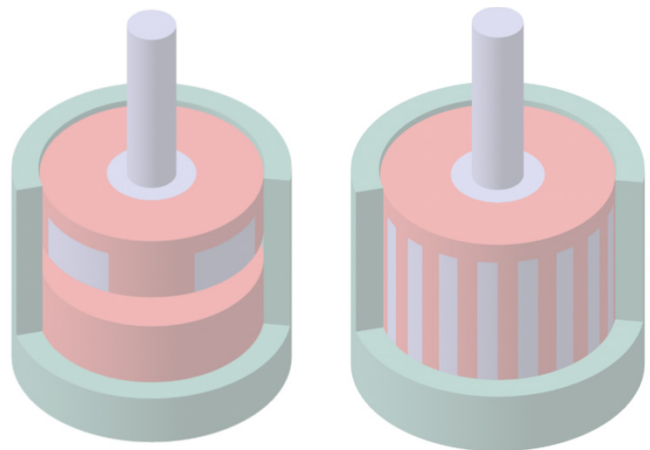


Fig. 7: (Colour on-line) Schematics of experiments designed to test the amplification mechanism caused by the modulation of magnetic permeability. In each drawing the pale-green outer cylinder can be made of stainless steel or copper, and the liquid metal is not represented. Left: a rotating disk is made of several sectors of alternating ferromagnetic and non-ferromagnetic materials. Liquid metal fills the space between this spinning disk and a bottom copper layer. Right: a thin layer of liquid metal is contained between two coaxial cylinders. The internal cylinder rotates and is made of alternating ferromagnetic and non-ferromagnetic materials.

Again the system is adjusted so that the surface is smooth, in order to reduce the drag exerted on the cylinders. A shear is localized in the gap between the cylinders when they rotate at different angular velocities.

In both setups, the shear is strong close to the permeability modulation and the conversion mechanism is likely to be efficient. Its efficiency will strongly depend on the structure of the boundary layers close to the rotating parts. Some tuning of the experiment may be required to achieve the optimal boundary layer thickness: it should be small, for the shear to be strong, but larger than the skin depth, for the small-scale magnetic field to penetrate deeply enough inside the fluid. By applying an azimuthal magnetic field and measuring the induced field normal to the modulated surface, it will be possible to quantify the conversion intensity. We expect to observe a large-scale field together with a component at the scale of the modulation. Their relative amplitudes will then be an indication of how effective the different steps of the conversion process described in figs. 5 and 6 are.

\*\*\*

We thank W. HERREMAN for stimulating discussions.

## REFERENCES

- [1] MOFFATT H. K., *Magnetic Field Generation in Electrically Conducting Fluids* (Cambridge University Press, Cambridge) 1978.

- [2] STIEGLITZ R. and MÜLLER U., *Phys. Fluids*, **13** (2001) 561.
- [3] GAILITIS A. *et al.*, *Phys. Rev. Lett.*, **86** (2001) 3024.
- [4] MONCHAUX R. *et al.*, *Phys. Rev. Lett.*, **98** (2007) 044502.
- [5] RAVELET F. *et al.*, *Phys. Rev. Lett.*, **101** (2008) 074502.
- [6] PÉTRÉLIS F., MORDANT N. and FAUVE S., *Geophys. Astrophys. Fluid Dyn.*, **101** (2007) 289.
- [7] GISSINGER C., *EPL*, **87** (2009) 39002.
- [8] LAGUERRE R. *et al.*, *Phys. Rev. Lett.*, **101** (2008) 104501.
- [9] BERHANU M. *et al.*, *EPL*, **77** (2007) 59001.
- [10] BERHANU M. *et al.*, *Eur. Phys. J. B*, **77** (2010) 459.
- [11] GIESECKE A., STEFANI F. and GERBETH G., *Phys. Rev. Lett.*, **104** (2010) 044503.
- [12] BUSSE F. H. and WICHT J., *Geophys. Astrophys. Fluid Dyn.*, **64** (1992) 135.
- [13] Similar modifications of the skin depth have been exemplified, for instance, in the Ponomarenko dynamo, see GILBERT A.D., *Geophys. Astrophys. Fluid Dyn.*, **44** (1972) 541.
- [14] LOWES F. J. and WILKINSON I., *Nature*, **198** (1963) 1158.